Cytokine Deposition Alters Leukocyte Morphology and Initial Recruitment of Monocytes and γδT Cells After Corneal Injury

Sonali Pal-Ghosh,[1] Ahdeah Pajoohesh-Ganji,[1] A. Sue Menko,[2] Hye-young Oh,[1] Gauri Tadvalkar,[1] Daniel R. Saban,[3] and Mary Ann Stepp[1]

[1]Department of Anatomy and Regenerative Biology and Department of Ophthalmology, The George Washington University Medical School, Washington, DC, United States
[2]Department of Pathology, Anatomy, and Cell Biology, Thomas Jefferson University, Philadelphia, Pennsylvania, United States
[3]Department of Ophthalmology and Immunology, Duke University School of Medicine, Durham, North Carolina, United States

Correspondence: Mary Ann Stepp, Department of Anatomy and Regenerative Biology, Department of Ophthalmology, The George Washington University Medical School, 2300 I Street NW, Washington, DC 20037, USA;
mastepp@gwu.edu.

Submitted: November 5, 2013
Accepted: March 12, 2014

Citation: Pal-Ghosh S, Pajoohesh-Ganji A, Menko AS, et al. Cytokine deposition alters leukocyte morphology and initial recruitment of monocytes and γδT cells after corneal injury. *Invest Ophthalmol Vis Sci*. 2014;55:2757–2765. DOI:10.1167/iovs.13-13557

Purpose. An in vivo mouse model reproducibly induces recurrent epithelial erosions in wild-type mice spontaneously 2 weeks after a single 1.5-mm corneal debridement wound made with a dulled blade. When 1.5-mm wounds are made by a rotating burr so that the corneal epithelial basement membrane is removed, corneas heal without developing erosions. Here, we characterize differences in cytokine deposition and changes in leukocytes between 0 and 6 hours after dulled-blade and rotating-burr wounding.

Methods. BALB/c mice were used to study 1.5-mm corneal wounds made using a dulled blade or a rotating burr. Mice were studied immediately after wounding (0 hour) and at 6 hours in vivo and in vitro in organ culture. Corneas, corneal extracts, and collagenase digests from naïve and wounded mice were used for three-dimensional (3D) confocal imaging, cytokine arrays, and flow cytometry.

Results. Confocal imaging showed CD45, a protein derived from leukocytes, accumulates at the wound edge by 3 and 6 hours after wounding in vivo but not in vitro with more CD45 accumulating after dulled-blade compared with rotating-burr wounds. Morphologic changes occurred in CD45+ leukocytes and higher levels for several cytokines were detected in the stromal wound bed within minutes following dulled-blade wounds. Flow cytometry showed significantly more monocytes (CD45+/CD11b+/Ly6C+) and γδT cells (CD45+/GL3+) recruited into the corneas of mice with dulled-blade wounds by 6 hours.

Conclusions. Differences in cytokine-driven leukocyte responses are seen after dulled-blade debridement compared with rotating-burr injury.

Keywords: mouse, monocytes, γδT cells, basement membrane, innate immune response

A recent study performed by the Cochrane Collaboration[1] looked at the current interventions used for treatment of recurrent erosions and concluded that we are "in need of additional high quality clinical trials to guide management of recurrent corneal erosions." Traumatic corneal abrasion is the leading cause of visits to the emergency room[2,3] and the incidence of recurrent erosions after corneal trauma has been estimated at 1 in every 150 cases.[4] While trauma accounted for approximately one-half of the cases of recurrent erosions in one study, epithelial membrane dystrophy was the cause in approximately one-third of the cases.[5] Treatments generally involve removing the epithelium mechanically by debridement, superficial keratectomy, or excimer laser. However, therapeutic contact lenses, anterior stromal puncture, oral tetracycline, and/or topical prednisolone have also been used with variable success.[1]

Alcohol delamination has been described as a treatment option for patients with recurrent erosions that aims to preserve the structure of the basement membrane.[6,7] Previously we showed that removing the basement membrane at the time of injury to the mouse cornea, either by manual keratectomy or using a rotating burr, enhanced long-term resolution of an intact epithelial barrier.[8,9] This suggests that treatment options for patients aimed at preserving the basement membrane intact might increase the likelihood of further erosions.

The rapid increase in leukocytes within the cornea after injury is due to induction of the innate immune response, which is regulated by the interaction of ligands with Toll-like receptors (TLRs) present on resident and recruited leukocytes.[10–13] Compared with microbial activation, the molecular events that activate the innate immune system after "sterile" wounding caused by trauma are poorly understood.[10,11] Exposure of resident cells in the epithelium and stroma to DNA and proteins from dead epithelial cells and the products made by commensal bacteria likely activate TLR signaling within resident and recruited leukocytes in the cornea after injury.

The basement membrane could reduce leukocyte activation by preventing cytokine-mediated signals from being delivered to resident leukocytes and allowing time for blinking and tears to reduce their concentrations. It could increase leukocyte

Copyright 2014 The Association for Research in Vision and Ophthalmology, Inc.

Downloaded from iovs.arvojournals.org on 04/24/2024

activation by acting as a sponge to retain cytokines and release them over time into the stroma. The impact of the basement membrane may vary depending on whether it is exposed or if epithelial cells have migrated over it, trapping adhered cytokines, and denatured matrix proteins. To begin to determine how the basement membrane contributes to erosion formation, short-term in vivo and organ culture experiments described were performed. The data obtained provide new insight into the roles cytokines play in the response of tissues to injury and immune cell recruitment.

Materials and Methods

Corneal Wound Healing

All studies performed comply with the George Washington University Medical Center Institutional Animal Care and Use Committee guidelines and with the ARVO Statement for the Use of Animals in Vision Research. Male BALB/c mice (NCI, Frederick, MD, USA) between the ages of 7 and 8 weeks were used for all of the experiments described. Mice were anesthetized with ketamine/xylazine and a topical anesthetic applied to their ocular surface. Unless stated otherwise, a 1.5-mm trephine was used to demarcate the wound area and the epithelial tissues within the area removed using either a dulled blade or a rotating burr (AlgerbrushII; Ambler Surgical, Exton, PA, USA) with a 0.5-mm burr tip. After wounding, mice were either euthanized immediately or erythromycin ophthalmic ointment was applied to the injured cornea and allowed to heal for 6 hours after which they were euthanized. The wounded corneas from mice euthanized immediately after wounding were used for organ culture, or fixed immediately for immunofluorescence (IF) studies. The numbers of corneas needed for each assay varied; all experiments were repeated 2 to 3 times.

Flow Cytometry

For flow cytometry studies, dulled-blade and rotating-burr wounded corneas were obtained 6 hours after wounding. Corneal buttons from both control and wounded mice were carefully dissected making sure to leave a minimal and uniform limbal rim. The corneal buttons were placed in ice-cold, serum-free media overnight. The numbers of corneas used per assay was six to eight per variable and experiments were repeated three times. The following day, corneas were digested with collagenase and released cells used for determination of immune cell subtypes as described previously.[14] The numbers of leukocytes present in the wounded corneas were compared with those present in naïve corneas.

Immunofluorescence and Whole Mounts

Whole-mount staining and confocal imaging for three-dimensional (3D) reconstruction was performed as described previously.[8] Whole-mount IF studies were performed on corneas from mice euthanized immediately after wounding; tissues were in fix within 5 minutes of injury; these are referred to as 0 hour time points. Mice were also allowed to heal for 3 and 6 hours prior to euthanization and their corneas used for whole-mount studies. Volocity (Perkin Elmer, Waltham, MA, USA) was used to obtain 3D renderings of confocal image stacks. For each variable a minimum of six corneas was assessed and the data presented are representative of those obtained. For quantitation of CD45 protein at the leading edge, images were acquired using the Zeiss Cell Observer Z1 spinning disk confocal microscope (Carl Zeiss, Inc., Thornwood, NY, USA), equipped with ASI MS-2000 (Applied Scientific Instrumentation, Eugene, OR, USA) scanning stage with z-galvo motor, and Yokogawa CSU-X1 spinning disk. A multi-immersion ×25/0.8 objective lens, LCI Plan-Neofluar, was used for imaging, with oil immersion. Evolve Delta (Photometrics, Tucson, AZ, USA) 512 × 512 EM-CCD camera was used as detector (80-msec exposure time). A diode laser emitting at 488 nm was used for excitation (54% power). Zen Blue software (Carl Zeiss, Inc.) was used to acquire the images, fuse the adjacent tiles, and produce maximum intensity projections. The adjacent image tiles were captured with overlap to ensure proper tiling. All images were acquired using the same intensity settings. The free form line tool in Image Pro Plus (Version 5.0; Media Cybernetics, Rockville, MD, USA) was used to quantify pixel intensities at the leading edge as defined by the presence of K14+ corneal epithelial cells. The intensity of CD45 was assessed 6 hours after wounding for six dulled-blade and seven rotating-burr corneas. For each cornea, the leading edges were traced three times and the average mean pixel intensity determined for each cornea.

For the morphometry studies, images were acquired using the Zeiss Cell Observer Z1 spinning disk confocal microscope as described above. A minimum of three corneas were used per variable for the morphometry studies unless otherwise specified. Negative controls were included for each study described and showed minimal background staining (data not shown).

Cytokine Arrays

The term cytokine is used throughout and includes proteins in the chemokine family. For cytokine array studies, mice were euthanized and epithelial tissues were obtained by limbal to limbal debridement using either dulled blade or rotating burr. Epithelial tissues were frozen immediately in liquid nitrogen. The de-epithelialized corneal stromal buttons were dissected maintaining a uniform thin limbal rim and immediately frozen in liquid nitrogen. Eight corneas were used for each variable and for each cytokine array study performed. De-epithelialized stromal buttons and epithelial tissues from dulled-blade and rotating-burr wounded corneas were extracted in radioimmunoprecipitation assay buffer containing protease inhibitors. Insoluble proteins were removed by microcentrifugation and the protein concentration of the supernatants determined. Equal micrograms of protein (160 μg) from each variable were used to perform cytokine arrays (#ARY020; R&D Systems, Minneapolis, MN, USA) according to manufacturer's instructions. Arrays were repeated three times. Each array generates duplicate values for each cytokine and the data presented in the Table shows the combined means of the four values for at least two experiments and are representative of all three experiments performed. A forth set of arrays were performed using tissues derived from mice wounded while under general and local anesthesia to determine whether different results were obtained if mice were alive at the time of injury. Cytokine array results were similar for mice euthanized immediately before or immediately after wounding (data not shown).

Organ Culture

Corneas were wounded and eyes enucleated and placed in serum free organ culture media prepared as described previously.[15] Eyes were incubated at 37°C, 7% CO_2 for 6 hours, after which the corneas were dissected and fixed for use in whole-mount IF studies.

Morphometry

All of the corneas used for morphometry studies were rapidly fixed in cold (–20°C) 70% methanol:30% dimethyl sulfoxide

Investigative Ophthalmology & Visual Science

Downloaded from iovs.arvojournals.org on 04/24/2024

Table. Cytokine Levels at the Time of Wounding Determined by Cytokine Array

	Stromal Tissue Only*		Harvested Epithelial Tissues†	
	RB	DB	RB	DB
CXCL1	**627 ± 25.9**	**866 ± 56.6**	***1110 ± 51.4***	***971 ± 21.4***
CX3CL1	—	31.1 ± 5.92	110 ± 14.5	56.4 ± 10.9
CXCL5	—	34.7 ± 15.7	—	—
CXCL11	—	—	—	—
CXCL12	—	53.9 ± 6.88	66.0 ± 10.3	59.3 ± 6.24
CXCL16	—	36.9 ± 14.0	***42.9 ± 7.65***	***17.5 ± 3.70***
CCL2	1471 ± 46.3	1490 ± 32.9	***2080 ± 82.0***	***1700 ± 21.5***
CCL6	2460 ± 51.9	2760 ± 49.9	***2570 ± 45.3***	***2050 ± 53.6***
CCL8	321 ± 51.0	356 ± 46.0	34.7 ± 11.8	—
CCL9/10	155 ± 13.2	190 ± 11.1	—	—
CCL11	—	—	—	—
CCL12	1770 ± 54.5	1930 ± 122	***1560 ± 35.4***	***2300 ± 44.4***
CCL21	**103 ± 29.1**	**230 ± 25.7**	—	—
CCL27	90.8 ± 5.37	75.6 ± 12.9	***182 ± 28.9***	***65.4 ± 6.10***
DF	1760 ± 162	2040 ± 53.5	626 ± 145	405 ± 113
IL16	1470 ± 33.5	1720 ± 108	***4980 ± 248***	***3090 ± 64.1***
Hspd1	**148 ± 13.6**	**215 ± 14.7**	446 ± 18.0	410 ± 17.9
C5	174 ± 43.8	241 ± 16.7	—	—
RARRES2	2800 ± 79.9	2750 ± 80.0	***1570 ± 137***	***619 ± 52.3***
GP130	**82.8 ± 23.8**	**204 ± 32.8**	—	—

The numerical values shown were obtained using NIH Image of films generated by chemiluminescence after cytokine arrays (see Materials and Methods). For each value shown, $n = 4$ data points from two different experiments. Values which were below detection are indicated by —. RB, rotating burr; DB, dulled blade.

* Samples were extracts of corneal stromal tissue remaining immediately after limbal-to-limbal debridement wounding with either the dulled blade or the rotating burr. Statistically significant differences in cytokines levels after wounding are shown in bold.

† Samples were extracts of epithelial tissues harvested at the time of limbal-to-limbal debridement wounding with either the dulled blade or the rotating burr. Statistically significant differences in cytokines levels after wounding are shown in italicized bold.

(vol/vol). This type of fixation was used to prevent changes in leukocyte morphology during tissue penetration by the fixative. There were no significant difference in the overall thicknesses of the stromas in the unwounded or wounded corneas 6 hours after wounding in vivo or in vitro. The stromal thicknesses ranged between 120 and 150 μm. Morphometry was performed using montaged z-stack images of the whole mounts of corneas stained to reveal CD45+ cells obtained from spinning disk microscope as described above. Since CD45 is a cell surface protein, IF images reveal the shapes of the CD45+ leukocytes within the stroma. To minimize variability, morphometry was performed at a standard distance (25 μm) from the posterior aspect of each cornea. A minimum of three, 1-μm z-sections from three different corneas were used for all variables assayed. From each image, 20 cells were randomly chosen for morphometry. Using ImageJ software (http://imagej.nih.gov/ij/; provided in the public domain by the National Institutes of Health, Bethesda, MD, USA), cell shapes were traced and quantified by outlining the borders of the CD45+ cells. The area, perimeter, and Feret's diameters of a total of a minimum of 60 cells were obtained for unwounded, wounded time 0, 6-hours in vivo, and 6-hour organ-cultured corneas. Feret's diameter is a commonly used term to describe particle shapes in microscopic data and is defined as the distance between two parallel tangential lines. Cells with longer more dendritic shapes have a larger perimeter and Feret's diameter. Statistical significance was determined by Student's *t*-test.

Antibodies

The following antibodies were used for immunofluorescence studies: CD45 (#553076; BD Pharmingen, San Jose, CA, USA), and K14 (#PRB-155P-100; Covance, Chantilly, VA, USA). The appropriate subclasses of secondary antibodies were obtained from either Molecular Probes (Grand Island, NY, USA) or Jackson Immunoscience (West Grove, PA, USA). The following antibodies were used for flow cytometry studies: LY6C Alexa 488 (CIHK1.4, #128022; BioLegend, San Diego, CA, USA), F4/80 PE (Cl BM8, #123118; BioLegend) LY6G PercpCy5.5 (1A8, 127616; Biolegend), CD11c PE Cy7 (CI HL3, #558079; BD Pharmingen), CCR2 APC (#FAB5538A; R&D Systems), CD45-APC Cy7 (CI 30-F11, #103116; BioLegend), and CD11b V500 (M1/70, #562127; BD Pharmingen). Also used was Fc block-Anti mouse CD16/32 (#14-0161-86; eBiosciences, San Diego, CA, USA).

Results

CD45 Accumulates at the Leading Edge Within 6 Hours After Wounding

Previously we showed that there were more CD45+ leukocytes in the stroma beneath the leading edge 6 hours after dulled-blade compared with rotating-burr wounding in vivo.[9] When epithelial cells at the margin of a debridement wound are ruptured at the time of injury, resident leukocytes clear the epithelial cell debris. To determine when CD45+ leukocytes accumulate at the leading edge, whole-mount IF studies were performed at 0 (wounded, euthanized immediately), 3-, and 6-hour time points. All corneas were fixed as described within 5 minutes of euthanization. Epithelial cells were localized with an antibody against K14, an epithelial keratin. For each variable presented in Figure 1, a minimum of six different corneas were assessed. Representative data from 3D confocal imaging analyses showed that at 0 hour, CD45 was present within the stroma and near the leading edges of both rotating-burr and dulled-blade wounded corneas (Fig. 1A). Also visible at 0 hour

Investigative Ophthalmology & Visual Science

Downloaded from iovs.arvojournals.org on 04/24/2024

IOVS | April 2014 | Vol. 55 | No. 4 | 2760

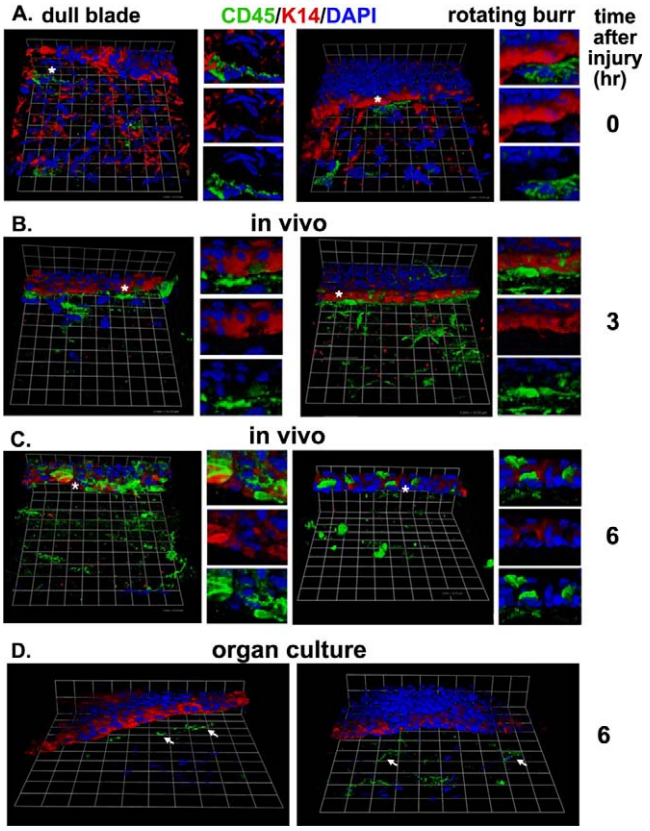

Figure 1. CD45 protein accumulates over time at the leading edge. (**A**) Data from 3D images generated by high-resolution confocal imaging show distorted 4′,6-diamidino-2-phenylindole (DAPI)–stained nuclei (*blue*) at the anterior surface of the exposed basement membrane and stroma within 5 minutes after injury. The epithelial cells at the leading edge are revealed by staining with keratin 14 (*red*). CD45+ leukocytes (*green*) are present in the anterior stromas of both dulled-blade and rotating-burr wounded corneas. K14 staining is more intense at the leading edge after rotating-burr wounds because epithelial cells accumulate at the wound edge when the burr is used. (**B**) CD45+K14 staining is seen at the leading edge 3 hours after both wound types with more leukocytes after rotating-burr wounds. Nuclei stained with DAPI are no longer seen at the anterior surface of the exposed stroma consistent with apoptosis of these cells. K14 is upregulated at the leading edge of both dulled-blade and rotating-burr wounds, but the difference is greater after dulled-blade wounds. In addition, CD45+ cells can be seen at the anterior stroma after both dulled-blade and rotating-burr wounds. (**C**) More CD45+K14 staining is present at the leading edge after dulled-blade wounds at the 6-hour time point. CD45+K14 staining can be seen on top of the epithelial cells especially after rotating-burr wounds. K14 continues to be more abundant at the leading edge after dulled-blade wounds. (**D**) When corneas are placed in organ culture after dulled-blade or rotating-burr wounds, CD45 staining is not seen at leading edge 6 hours after wounding. *Squares* are 19.35 μm.

were the distorted nuclei of the anterior stromal cells and debris from lysed K14+ epithelial cells on the anterior stroma. More K14+ debris remains after dulled-blade wounding.

By 3 and 6 hours, CD45 protein had accumulated adjacent to and beneath K14+ epithelial cells at the leading edge of both wound types (Figs. 1B, 1C). Anterior stromal nuclei and K14 debris on the exposed stromal surface were no longer present. These representative images suggest that by 6 hours, more CD45 protein was present at the leading edge after dulled-blade wounding. An additional seven rotating-burr and six dulled-blade wounded corneas obtained 6 hours after wounding were used to quantify CD45 pixel intensities at the leading

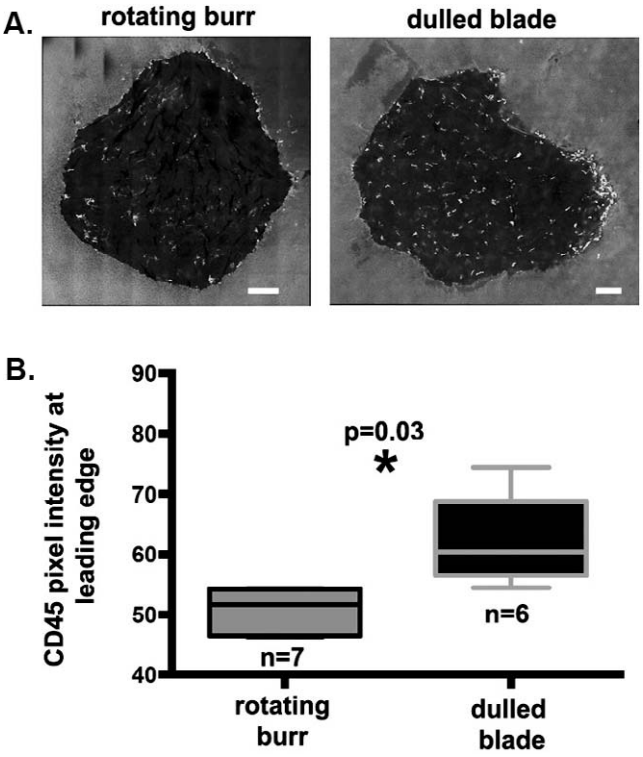

Figure 2. Quantitation of CD45 confirms that more leukocyte-specific protein is present at the leading edge 6 hours after dulled-blade compared with rotating-burr wounds. (**A**) Representative montaged z-sections obtained showing CD45 protein at the leading edge 6 hours after dulled-blade and rotating-burr wounds. In total, seven and six corneas were used for quantitation of CD45 after rotating-burr and dulled-blade wounds. (**B**) Mean pixel intensity values for CD45 were determined at the leading edge. CD45 was found to be significantly more abundant at the leading edge after the dulled-blade wounds. *Scale bars*: 170 μm.

edge. Figure 2A shows representative flat-mount montaged images showing the localization of CD45 protein at the leading edge. Quantitation of these images was performed using Image Pro Plus software as described in the methods section and results are shown in Figure 2B; there is significantly more CD45 protein accumulated at the leading edge by 6 hours after dulled-blade compared with rotating-burr wounds.

When wounded mice were euthanized immediately after injury and their corneas placed in organ culture for 6 hours, CD45 protein was not detected at the leading edge, within, or on top of the corneal epithelium (Fig. 1D). Organ culture denervates the cornea by severing the nerves and prevents recruitment of leukocytes from the tear film and limbal vasculature. These results indicate that the deposition of CD45+ protein at the leading edge observed in vivo at 3 and 6 hours after wounding does not occur ex vivo in organ culture.

Wound Type–Specific Differences in Morphology of Resident Stromal Leukocytes Detected Within Minutes of Injury

The images presented in Figures 1 and 2 suggest differences in leukocyte deposition at the leading edge in vivo compared with in vitro as well as differences in leukocyte morphology in the anterior stroma 6 hours after dulled-blade wounding. We next quantified stromal leukocyte morphology in naïve and in corneas minutes after wounding. Data were then compared with those obtained 6 hours after wounding in vivo and in

Investigative Ophthalmology & Visual Science

Downloaded from iovs.arvojournals.org on 04/24/2024

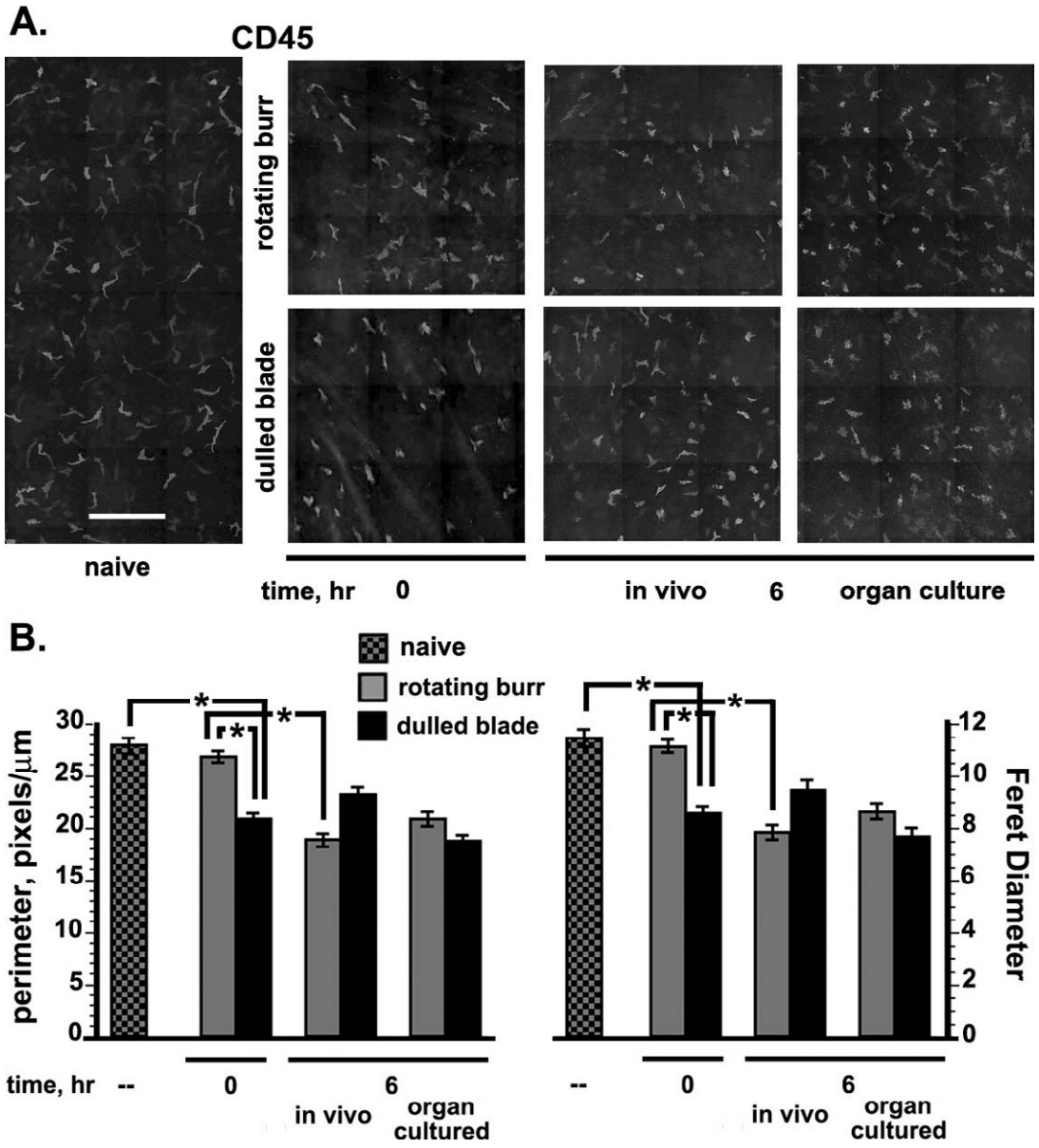

FIGURE 3. Resident immune cell morphology changes occur within minutes of wounding. (**A**) Representative montaged z-sections 25 μm from the posterior aspect of the cornea from flat-mounted tissues stained to reveal CD45+ leukocytes. Cell shapes were determined by morphometry from 20 randomly selected cells from images taken from a minimum of three different corneal stromas for each variable assessed using ImageJ and data for perimeters and Feret's Diameter are presented in (**B**). *Asterisks* indicate statistical significance determined by ANOVA ($P < 0.05$). *Scale bar* (**A**): 200 μm.

corneas placed in organ culture. To eliminate differences in the rate of penetration of fixative from impacting leukocyte morphology, corneas were fixed by rapid immersion in −20°C methanol. Leukocytes in the mouse corneal stroma are stratified in the naïve mouse such that dendritic cells are found in the anterior stroma and monocytes and macrophages in the posterior stroma.[16–18] Morphometry was performed at a standard distance (25 μm) from the posterior aspect of the cornea. Cell shapes were quantified by measuring perimeters and calculating their Feret's diameter as described in the Methods section; cells with more dendritic shapes have larger perimeters and correspondingly larger Feret's diameters. Representative images are shown in Figure 3A and quantitative data for cell perimeters and Feret's diameter are presented in Figure 3B.

The mean perimeter and Feret's diameter was 27.8 ± 0.8 SEM pixels/μm and 11.4 ± 0.33 SEM, respectively, for CD45+ leukocytes from naïve unwounded corneas. These values are greater than those seen after wounding for all the variables tested except for 0 hour after rotating burr where the mean perimeter and Feret's diameter was 26.7 ± 0.6 SEM pixels/μm and 11.1 ± 0.25 SEM, respectively. By contrast, the values for mean perimeter and Feret's diameter for leukocytes at the 0 hour time point after dulled-blade wounds were significantly less at 20.8 ± 0.53 SEM pixels/μm and Feret's Diameter was 8.6 ± 0.22 SEM, respectively. Within minutes after injury, leukocytes in the dulled-blade wounded stromas are less dendritic than those in the rotating-burr wounds.

For dulled-blade wounds leukocyte morphologies do not change significantly after time 0: values are the same at 6 hours in vivo and in vitro compared with 0 hour. By contrast, leukocytes in the stromas of rotating-burr wounded corneas were significantly more round 6 hours after wounding in vivo and in vitro compared with the 0 hour time point.

Investigative Ophthalmology & Visual Science

Downloaded from iovs.arvojournals.org on 04/24/2024

In summary, these data demonstrate that leukocytes assume more rounded shapes following wounding compared with leukocytes in naïve corneas. The change in leukocyte morphology seen after dulled-blade wounding was maximal within minutes after injury; no further change was seen compared with 0 hour by 6 hours after wounding in vivo or in vitro. Changes in leukocyte morphology after rotating-burr wounds took longer and do not require factors present in vivo since they also occur in organ culture.

Mice Wounded With the Dulled Blade Have Elevated Levels of Several Cytokines in Their Stroma

Cytokines, a large class of small proteins that includes chemokines, are considered responsible for the activation and recruitment of leukocytes after injury.[11,13,19] While cytokines are released from resident and recruited leukocytes, corneal keratocytes and epithelial cells also produce them. The increased CD45+ protein at (Figs. 1, 2) and beneath[9] the wound edge at 6 hours in vivo after dulled-blade wounds and the differences in leukocyte morphology that arise immediately after dulled-blade wounding shown in Figure 3 suggest differences in cytokine levels on the corneal stroma after the two wound types.

To examine this question, we performed chemokine array studies on protein extracts obtained from corneal stromas and epithelia immediately following dulled-blade and rotating-burr wounding. Epithelial tissues were harvested by limbal to limbal dulled-blade or rotating-burr wounding; denuded stromas were dissected. Tissues were extracted and used for cytokine array experiments as described in the methods section. The Table shows the means for all of the cytokine array data obtained. The levels of several cytokines including CX3CL1, CXCL5, CXCL12, and CXCL16 were below detectable in corneal stromas wounded with the rotating burr, but detectable in the stromas of dulled-blade wounded corneas. CXCL1 and CCL21 were significantly higher in the stromas of dulled-blade wounded corneas. No cytokines were significantly higher in the stromas of corneas wounded by rotating burr. GP130, a component of the IL6 family of cytokine receptors, and Hspd1, a heat-shock protein, were also elevated significantly in dulled-blade compared with rotating-burr stromas. Importantly, the levels of several cytokines were the same in these stromal extracts; these include CCL2, CCL6, CCL8, CCL9/10, CCL12, CCL27, IL16, RARRES2, as well as complement factors 5 and D. The significant differences seen in specific cytokine levels were not due to differences in the amounts of stromal extracts used for these assays.

If fewer cytokines were left behind on the rotating-burr stromas, cytokine levels would be expected to be higher in the epithelial tissues removed by the rotating burr. There were significantly elevated levels for seven cytokines in the rotating-burr epithelial extracts, including CXCL1, CXCL16, CCL2, CCL6, CCL27, IL6, and RARRES2, and similar levels for four, including CX3CL1, CXCL12, Hspd1, and complement factor D. One cytokine (CCL8) was below detectable in the epithelial cells removed by dulled-blade wounding but present at in rotating-burr epithelial tissues.

The array data presented in the Table were obtained from mice euthanized immediately prior to injury. A separate array study was performed using tissues derived from mice wounded while under general and local anesthesia and euthanized immediately after wounding to determine whether results varied if mice were alive at the time of injury. Cytokine array results were similar for mice euthanized immediately before or immediately after wounding (data not shown).

These data confirm that immediately after dulled-blade compared with rotating-burr wounds, specific cytokines are present on the stroma at higher levels. The fact that four cytokines were only found in the dulled-blade and not in the rotating-burr stromas immediately after injury provides further support for this conclusion.

More Monocytes and γδT Cells Are Recruited Into the Cornea After Dulled-Blade Wounds

To determine the identities of the leukocytes rapidly recruited into the corneas, we performed flow cytometry studies 6 hours after dulled-blade and rotating-burr injury. Figure 4A shows the gating scheme used for flow studies. Compared with naïve corneas, 30- and 47-fold more CD45+/Ly6C hi/Ly6G+/CD11b hi/F480 low/CD11c+ monocytes (Fig. 4B) were present 6 hours after rotating-burr and dulled-blade wounds, respectively. In addition, we found a 2.6- and 6.2-fold increase in CD45-gated GL3+ γδT cells (Fig. 4C) 6 hours after rotating-burr and dulled-blade wounds, respectively. The increases seen in CD45+Ly6C hi monocytes and in CD45-gated GL3+ γδT cells in corneas wounded by dulled blade were significantly greater than those for the rotating burr. More neutrophils and dendritic cells were also present in wounded corneas at 6 hours compared with controls, but no significant differences were detected between wound types (data not shown). Increased levels of CXCL1 and CCL21 seen in the stromas after dulled-blade wounds correlate with induced recruitment of more monocytes and γδT cells 6 hours after injury.

Discussion

Our data show that the initial activation and recruitment of leukocytes after both rotating-burr and dulled-blade wounding are events that take place rapidly. Within minutes of dulled-blade injury, leukocyte shape changes are seen in resident cells in the exposed stroma with cells rounder after dulled-blade compared with naïve and rotating-burr wounded corneas. Cytokine array studies show more cytokines are left on the stroma after dulled-blade wounding. Within 6 hours, increased recruitment of monocytes and γδT cells are observed in dulled-blade wound corneas. Since rotating-burr wounded corneas that lack a basement membrane resolve their injuries, but dulled-blade wounded corneas go on to develop recurrent erosions,[9] these studies provide important insight in several key events triggered within hours after corneal wounding.

Rapid Changes in Leukocyte Morphology

We show here for the first time that CD45+ leukocytes in the corneal stroma change their morphology within minutes to become more round after dulled-blade corneal wounding. These differences in leukocyte morphology are not due to fixation artifacts or to differences in corneal swelling. A limitation of our studies was the use of CD45 to calculate leukocyte perimeters and Feret's Diameter. Brissette-Storkus and colleagues[20] documented the presence of a mixed population of resident monocytes and macrophages in the naïve mouse cornea using CD45. Their studies showed that "virtually all" of the CD45+ cells in the stroma also express CD11b and 52% of the CD45+CD11b+ cells expressed F4/80. Of the cells expressing F4/80, 50% also expressed MHC class II indicating that they are dendritic cells. Hamrah and colleagues[18] showed that dendritic cells are primarily localized to the anterior stroma beneath the corneal epithelium and monocytes and macrophages were located in the posterior stroma where we quantified leukocyte shapes. Thus, the

Investigative Ophthalmology & Visual Science

Downloaded from iovs.arvojournals.org on 04/24/2024

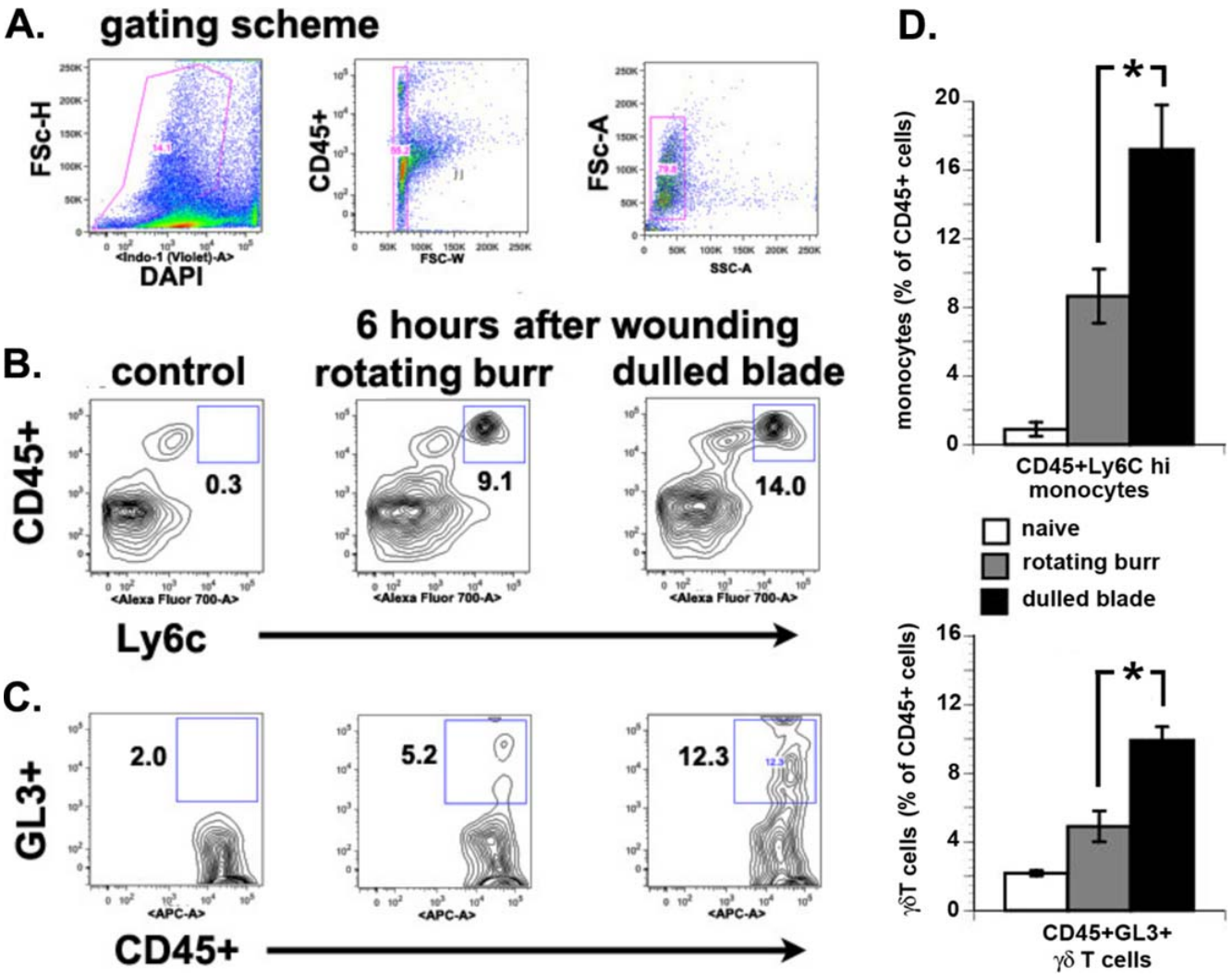

FIGURE 4. Flow cytometry shows more CD45+Ly6C hi monocytes and γδT cells recruited into the cornea after dulled-blade wounds. Flow cytometric characterization of inflammatory cell populations in RB compared with DB wounds. Cells were isolated from dissected corneas 6 hours after RB and DB wounding using collagenase. (**A**) Gating scheme to eliminate background 'noise.' Dead cells (DAPI+), cell clumps (FSc-W), and cell debris (SSC-A) were gated out, and remaining events were used for the phenotypic analyses indicated. (**B**) Characterization of infiltrated monocytes (CD45+Ly6C hi). (**C**) Characterization of GL3+CD45+ γδT cells. (**D**) There are more CD45+Ly6c-hi monocytes and GL3+CD45+ γδT cells after both wound types. However, based on three independent assessments, the percentage of CD45+ cells that are Ly6c-hi and GL3+ is significantly greater after dulled-blade compared with rotating-burr wounds.

CD45+ cells undergoing shape changes within minutes of dulled-blade injury are located where monocytes and macrophages are found.

Resident monocytes and macrophages pass through several stages during their activation from responsive, to primed, and then to the fully activated state[21] with priming and activation generally taking place over a time frame of 1 to 24 hours.[22–24] Studies using lipopolysaccharide or mechanical forces to activate responsive leukocytes in vitro induce cell spreading[22,23,25] and increase cell perimeters and Feret's diameter. Naïve leukocytes imaged at the same location in the stroma were significantly more elongated compared with leukocytes immediately after dulled-blade wounding. Based on timing and morphology, these data are consistent with conversion of monocytes and macrophages from the resident to responsive state. Additional studies looking at the functions of isolated leukocytes immediately after both wound types in vitro will be required to determine whether this is the case.

We hypothesize that corneal injury causes a rapid shift in stromal leukocytes from the resident, well-spread, state to a responsive, more rounded, state that would enhance their migration. Since the leukocytes in dulled blade wounded stromas show more dramatic changes in their morphology, the cytokines present at higher levels in the dulled-blade wounded corneal stroma contribute more to these events than mechanical forces, which are greater during rotating-burr wounding.

The Rotating Burr Removes More Cytokines From the Exposed Stromal Surface

Cytokine array studies were performed on dulled-blade and rotating-burr wounded mouse corneal epithelial and stromal tissues immediately after injury. The rationale for these experiments was to determine whether differences in cytokine deposition at the time of injury contributed to the significant differences in leukocyte shape immediately after dulled-blade injury and to erosion formation. The results show that more cytokines were left on stromas after dulled-blade wounding and that more cytokines were removed along with epithelial tissues with the rotating burr. Transmission electron micros-

Investigative Ophthalmology & Visual Science

Downloaded from iovs.arvojournals.org on 04/24/2024

copy studies have shown that the basal surface of the basal epithelial cells with hemidesmosomes and α6β4 integrin remained on the exposed stroma over the intact basement membrane.[26] Keratin intermediate filaments, actin, and DNA from lysed epithelial cells must also be present. Because the rotating burr functions like a spindle, it removes cell debris more efficiently than does the dulled blade. The events described here take place during the first minutes to hours after corneal injury; they are likely to be driven by the cytokines present in the cellular debris sticking to the basement membrane. The increased retention of cytokines on the dulled-blade anterior stroma coupled with the rapidity of the changes in leukocyte morphology implicate cytokines in mediating the initial differential recruitment of monocytes and γδT cells into the stroma.

Increased Recruitment of Monocytes and γδT Cells After Dulled-Blade Wounds

Within 6 hours, we see enhanced recruitment of monocytes and γδT cells after dulled-blade wounding. Cytokine array studies provide a rationale for the differences in leukocytes observed. Dulled-blade wounding leaves more cytokines behind on the basement membrane; the rotating burr removes more cytokines from the corneal surface than does the dulled blade. Cytokines are responsible for both recruiting and activating leukocytes in vivo and in vitro. Chemokines have been divided into several families based on structure with CC and CXC chemokines making up two major families.[27,28] Three CXC chemokines (CXCL5, CXCL12, and CXCL16) as well as CX3CL1 were present in detectable levels in dulled-blade stromas but not rotating-burr stromas. In addition, elevated levels of CXCL1 and CCL21 were seen on the stroma after dulled-blade compared with rotating-burr wounds.

CXCL1 has been shown to induce neutrophil and T-cell recruitment[29–32] and CCL21 has been shown to induce T-cell and dendritic cell recruitment.[31,33] CXC chemokines have been associated with neutrophil recruitment, CC chemokines with monocyte and dendritic cell recruitment and macrophage activation, and CX3CL1 with monocyte and T-cell recruitment.[29,30] The differences in the cytokines seen here predict differences will emerge over time in the recruitment of leukocytes. Leukocytes play a critical role in mediating the wound response in the cornea and impact re-epithelialization and wound resolution.[34–42] Mice lacking different types of leukocytes have been used to study corneal wound healing responses and data show that neutrophils,[33–36] dendritic cells,[37,38] γδT cells,[39,40] and natural killer cells[38,41] all play roles in mediating the appropriate healing of the cornea after wounding. The importance of leukocytes also includes regulation of proper reinnervation by the sensory nerves.[42,43]

Most studies performed to look at innate responses involve use of microbes and microbial products.[10–13] These models induce an immune response that causes substantial tissue damage compared with that induced by "sterile" corneal injury. Our studies using two different methods for creating 1.5-mm corneal wounds reveal differences in the early response of the cornea to injury and indicate that not all "sterile" injuries activate the innate immune system similarly. Whether differences in the early recruitment of leukocytes drives erosion formation is not clear. Additional studies are needed to determine the signal(s) that induce and sustain the innate immune response to "sterile" injury and the mouse cornea is an excellent model to use to address these issues. The data presented highlight our need to understand the roles that both cytokine release and tissue damage play in the activation of the innate immune response after corneal injury.

Acknowledgments

The authors thank Anastas Popratiloff, PhD, director of the George Washington University Center for Microscopy and Image Analysis, for help with imaging. Site research was performed at the Department of Anatomy and Regenerative Biology and Department of Ophthalmology, The George Washington University Medical School, Washington, DC, United States.

Supported by the National Institutes of Health (NIH; Bethesda, MD, USA) SIG Grant F10 RR025565 for the Zeiss 710 confocal microscopy, and the Zeiss Cell Observer Z1 spinning disk confocal microscopy by a grant from NIH Office of the Director, 1S10OD010710-01. Also supported by NIH Grants EY08512 (MAS) and EY021784 (MAS, ASM).

Disclosure: **S. Pal-Ghosh**, None; **A. Pajoohesh-Ganji**, None; **A.S. Menko**, None; **H.-Y. Oh**, None; **G. Tadvalkar**, None; **D.R. Saban**, None; **M.A. Stepp**, None

References

1. Watson SL, Lee MH, Barker NH. Interventions for recurrent corneal erosions. *Cochrane Database Syst Rev*. 2012; CD001861.
2. Laibson PR. Recurrent corneal erosions and epithelial basement membrane dystrophy. *Eye Contact Lens*. 2010;36:315–317.
3. Jones NP, Hayward JM, Khaw PT, Claoué CM, Elkington AR. Function of an ophthalmic "accident and emergency" department: results of a six month survey. *Br Med J (Clin Res Ed)*. 1986;292:188–190.
4. Jackson H. Effect of eye-pads on healing of simple corneal abrasions. *Br Med J*. 1960;2:713.
5. Reidy JJ, Paulus MP, Gona S. Recurrent erosions of the cornea: epidemiology and treatment. *Cornea*. 2000;19:767–771.
6. Dua HS, Lagnado R, Raj D, et al. Alcohol delamination of the corneal epithelium: an alternative in the management of recurrent corneal erosions. *Ophthalmology*. 2006;113:404–411.
7. Singh RP, Raj D, Pherwani A, et al. Alcohol delamination of the corneal epithelium for recalcitrant recurrent corneal erosion syndrome: a prospective study of efficacy and safety. *Br J Ophthalmol*. 2007;91:908–911.
8. Pal-Ghosh S, Tadvalkar G, Jurjus RA, Zieske JD, Stepp MA. BALB/c and C57BL6 mouse strains vary in their ability to heal corneal epithelial debridement wounds. *Exp Eye Res*. 2008;87:478–486.
9. Pal-Ghosh S, Pajoohesh-Ganji A, Tadvalkar G, Stepp MA. Removal of the basement membrane enhances corneal wound healing. *Exp Eye Res*. 2011;93:927–936.
10. Barton GM. A calculated response: control of inflammation by the innate immune system. *J Clin Invest*. 2008;118:413–420.
11. Modlin RL. Innate immunity: ignored for decades, but not forgotten. *J Invest Dermatol*. 2012;132:882–886.
12. Lambiase A, Micera A, Sacchetti M, Mantelli F, Bonini S. Toll-like receptors in ocular surface diseases: overview and new findings. *Clin Sci (Lond)*. 2011;120:441–450.
13. Narayanan S, Redfern RL, Miller WL, Nichols KK, McDermott AM. Dry eye disease and microbial keratitis: is there a connection? *Ocul Surf*. 2013;11:75–92.
14. Hattori T, Chauhan SK, Lee H, et al. Characterization of Langerin-expressing dendritic cell subsets in the normal cornea. *Invest Ophthalmol Vis Sci*. 2011;52:4598–4604.
15. Stepp MA, Spurr-Michaud S, Gipson IK. Integrins in the wounded and unwounded stratified squamous epithelium of the cornea. *Invest Ophthalmol Vis Sci*. 1993;34:1829–1844.
16. Knickelbein JE, Watkins SC, McMenamin PG, Hendricks RL. Stratification of antigen-presenting cells within the normal cornea. *Ophthalmol Eye Dis*. 2009;1:45–54.

Investigative Ophthalmology & Visual Science

Downloaded from iovs.arvojournals.org on 04/24/2024

17. Guthoff RF, Zhivov A, Stachs O. In vivo confocal microscopy, an inner vision of the cornea - a major review. *Clin Experiment Ophthalmol*. 2009;37:100–117.
18. Hamrah P, Liu Y, Zhang Q, Dana MR. Alterations in corneal stromal dendritic cell phenotype and distribution in inflammation. *Arch Ophthalmol*. 2003;121:1132–1140.
19. Wilson SE, Mohan RR, Mohan RR, Ambrósio R Jr, Hong J, Lee J. The corneal wound healing response: cytokine-mediated interaction of the epithelium, stroma, and inflammatory cells. *Prog Retin Eye Res*. 2001;20:625–637.
20. Brissette-Storkus CS, Reynolds SM, Lepisto AJ, Hendricks RL. Identification of a novel macrophage population in the normal mouse corneal stroma. *Invest Ophthalmol Vis Sci*. 2002;43:2264–2271.
21. Adams DO, Hamilton TA. The cell biology of macrophage activation. *Annu Rev Immunol*. 1984;2:283–318.
22. Miyazaki H, Hayashi K. Effects of cyclic strain on the morphology and phagocytosis of macrophages. *Biomed Mater Eng*. 2001;11:301–309.
23. Shiratsuchi H, Basson MD. Extracellular pressure stimulates macrophage phagocytosis by inhibiting a pathway involving FAK and ERK. *Am J Physiol Cell Physiol*. 2004;286:C1358–C1366.
24. Gross S, Gammon ST, Moss BL, et al. Bioluminescence imaging of myeloperoxidase activity in vivo. *Nat Med*. 2009;15:455–461.
25. Yun Y, Han S, Park E, et al. Immunomodulatory activity of betulinic acid by producing pro-inflammatory cytokines and activation of macrophages. *Arch Pharm Res*. 2003;26:1087–1095.
26. Sta Iglesia DD, Stepp MA. Disruption of the basement membrane after corneal débridement. *Invest Ophthalmol Vis Sci*. 2000;41:1045–53.
27. Le Y, Zhou Y, Iribarren P, Wang J. Chemokines and chemokine receptors: their manifold roles in homeostasis and disease. *Cell Mol Immunol*. 2004;1:95–104.
28. Ono SJ, Nakamura T, Miyazaki D, Ohbayashi M, Dawson M, Toda M. Chemokines: roles in leukocyte development, trafficking, and effector function. *J Allergy Clin Immunol*. 2003;111:1185–1199.
29. Lin M, Carlson E, Diaconu E, Pearlman E. CXCL1/KC and CXCL5/LIX are selectively produced by corneal fibroblasts and mediate neutrophil infiltration to the corneal stroma in LPS keratitis. *J Leukoc Biol*. 2007;81:786–792.
30. Amescua G, Collings F, Sidani A, et al. Effect of CXCL-1/KC production in high risk vascularized corneal allografts on T cell recruitment and graft rejection. *Transplantation*. 2008;85:615–625.
31. Chintakuntlawar AV, Chodosh J. Chemokine CXCL1/KC and its receptor CXCR2 are responsible for neutrophil chemotaxis in adenoviral keratitis. *J Interferon Cytokine Res*. 2009;29:657–666.
32. Araki-Sasaki K, Tanaka T, Ebisuno Y, et al. Dynamic expression of chemokines and the infiltration of inflammatory cells in the HSV-infected cornea and its associated tissues. *Ocul Immunol Inflamm*. 2006;14:257–266.
33. Jin Y, Shen L, Chong EM, et al. The chemokine receptor CCR7 mediates corneal antigen-presenting cell trafficking. *Mol Vis*. 2007;13:626–634.
34. Li Z, Burns AR, Smith CW. Two waves of neutrophil emigration in response to corneal epithelial abrasion: distinct adhesion molecule requirements. *Invest Ophthalmol Vis Sci*. 2006;47:1947–1955.
35. Li Z, Burns AR, Rumbaut RE, Smith CW. γδT cells are necessary for platelet and neutrophil accumulation in limbal vessels and efficient epithelial repair after corneal abrasion. *Am J Pathol*. 2007;171:838–845.
36. Petrescu MS, Larry CL, Bowden RA, et al. Neutrophil interactions with keratocytes during corneal epithelial wound healing: a role for CD18 integrins. *Invest Ophthalmol Vis Sci*. 2007;48:5023–5029.
37. Gao N, Yin J, Yoon GS, Mi QS, Yu FS. Dendritic cell-epithelium interplay is a determinant factor for corneal epithelial wound repair. *Am J Pathol*. 2011;179:2243–2253.
38. Gao Y, Li Z, Hassan N, et al. NK cells are necessary for recovery of corneal CD11c+ dendritic cells after epithelial abrasion injury. *J Leukoc Biol*. 2013;94:343–351.
39. Byeseda SE, Burns AR, Dieffenbaugher S, Rumbaut RE, Smith CW, Li Z. ICAM-1 is necessary for epithelial recruitment of γδ T cells and efficient corneal wound healing. *Am J Pathol*. 2009;175:571–579.
40. Li Z, Burns AR, Miller SB, Smith CW. CCL20, γδ T cells, and IL-22 in corneal epithelial healing. *FASEB J*. 2011;25:2659–2668.
41. Liu Q, Smith CW, Zhang W, Burns AR, Li Z. NK cells modulate the inflammatory response to corneal epithelial abrasion and thereby support wound healing. *Am J Pathol*. 2012;181:452–462.
42. Li Z, Burns AR, Han L, Rumbaut RE, Smith CW. IL-17 and VEGF are necessary for efficient corneal nerve regeneration. *Am J Pathol*. 2011;178:1106–1116.
43. Sarkar J, Chaudhary S, Jassim SH, et al. CD11b+GR1+ myeloid cells secrete NGF and promote trigeminal ganglion neurite growth: implications for corneal nerve regeneration. *Invest Ophthalmol Vis Sci*. 2013;54:5920–5936.

Investigative Ophthalmology & Visual Science

Downloaded from iovs.arvojournals.org on 04/24/2024